

Multiboson production in W' decays

J. A. Aguilar–Saavedra^a, F. R. Joaquim^b

^a Departamento de Física Teórica y del Cosmos, Universidad de Granada,
E-18071 Granada, Spain

^b Departamento de Física and CFTP, Instituto Superior Técnico, Universidade de Lisboa,
Lisboa, Portugal

Abstract

In models with an extra $SU(2)_R$ gauge group and an extended scalar sector, the cascade decays of the W' boson can provide various multiboson signals. In particular, diboson decays $W' \rightarrow WZ$ can be suppressed while $W' \rightarrow WZX$, with X one of the scalars present in the model, can reach branching ratios around 4%. We discuss these multiboson signals focusing on possible interpretations of the ATLAS excess in fat jet pair production.

1 Introduction

A 3.4σ local excess in boson-tagged jet pair (JJ) production reported by the ATLAS Collaboration [1], near an invariant mass $m_{JJ} = 2$ TeV, stands out as the most prominent anomaly that the first run of the Large Hadron Collider (LHC) has left. This excess appears in a dedicated search for heavy resonances decaying into two gauge bosons WZ that subsequently decay hadronically, each boson resulting in one fat jet (J). The CMS analysis of the same JJ final state [2] also shows some excess at roughly the same invariant mass. But, intriguingly, complementary searches in the $\ell\nu J$ channel, corresponding to the leptonic decay $W \rightarrow \ell\nu$ ($\ell = e, \mu$) and Z hadronic decay, give null results [3, 4], even if — as in the case of the ATLAS search — they are more sensitive to the presence of a resonance. Consequently, the limits from the non-observation of a signal in this decay mode are in tension with the cross section required to explain the excess in ref. [1]. The $\ell^+\ell^-J$ channel with $Z \rightarrow \ell^+\ell^-$ and W decaying hadronically is less sensitive. In the case of the CMS Collaboration [3] there is some $\sim 2\sigma$ excess at a smaller invariant mass $m_{\ell\ell J} \sim 1.8$ TeV but the ATLAS analysis [5] gives a SM-like result. In addition, heavy resonances decaying into two gauge bosons VV ($V = W, Z$) are also expected to decay into Vh^0 , with h^0 the Higgs boson. Searches for Vh^0 in the JJ channel by the CMS Collaboration [6] do not show any excess, while a preliminary Wh^0 resonance search in the $\ell\nu J$ final state [7], less sensitive than the former, yields a 2.2σ excess at $m_{Wh^0} = 1.8$ TeV (see ref. [8] for a detailed discussion).

In order to address the tension between the ATLAS diboson excess [1] in the JJ channel and the limits on a possible signal from the other channels [2–5], the hypothesis that this excess is due to diboson production plus an extra particle X was put forward by one of us [8]. Two production and decay topologies were identified, with a heavy resonance R decaying into VVX via an intermediate on-shell resonance Y , as depicted in figure 1. In both cases, the VVX final state could give a diboson-like signal in the ATLAS analysis [1], while not showing up so conspicuously in the rest of diboson resonance searches. In this paper we present an explicit example of a model where such processes can occur, with R a charged spin-1 boson (W'), Y a charged (H^\pm) or neutral (H_1^0) scalar and X a pseudo-scalar (A^0) or the Higgs boson (h^0). Key ingredients in the model are an additional $SU(2)'$ gauge group, whose charged member is the W' boson, and an additional scalar doublet to provide the scalars H^\pm , H^0 and A^0 .

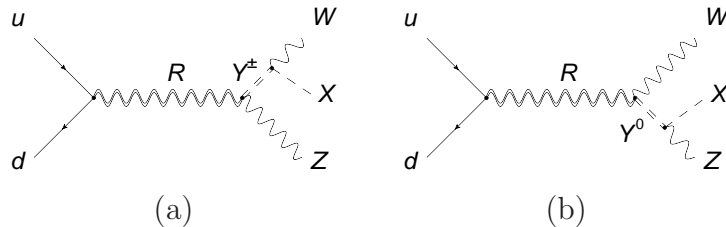


Figure 1: Sample diagrams for $R \rightarrow VY \rightarrow VVX$ production, with X a neutral scalar.

We note that many interpretations of the ATLAS excess in terms of a spin-1 resonance decaying into WZ , WW or ZZ have appeared in the literature [9], several with an extended scalar sector that couples to $SU(2)_L$ as well as to a new $SU(2)'$ gauge group. This is the case, for example, of left-right (LR) models. However, only direct decays $R \rightarrow VV$ have been considered, overlooking the tension between the JJ and $\ell\nu J$ analyses or attributing it to statistical fluctuations.¹ Direct $R \rightarrow JJ$ decays have also been considered in interpretations in terms of a new spin-0 resonance [16] and other related work [17]. As we will show in this paper, if the extra scalars present in models with an extra $SU(2)'$ symmetry group are lighter than the W' boson, their cascade decays can provide multiboson signals. An alternative explanation of the absence of signals in the $\ell\nu J$ final state is that the diboson excess is due to some new particle having a mass close to the W and Z masses, with hadronic decays, as proposed for example in ref. [18]. Nevertheless, this hypothesis does not explain why a significant excess has not been seen by the CMS Collaboration in their JJ resonance search.

¹Recently, the tension between the JJ excess and the SM-like results in the rest of ATLAS diboson searches has been numerically quantified [10], and amounts to 2.9 standard deviations. Preliminary results from the second run at 13 TeV leave no significant excess either [11–15], with a mild 1σ enhancement over the SM prediction near 2 TeV in the ATLAS JJ search.

In the remainder of this paper, we will first present in section 2 the models to be used as a framework. Multiboson W' decays will be discussed in section 3, focusing on the dependence of the different (diboson, triboson) signals on the mixing in the scalar sector of the model. The possible multiboson cross sections will be investigated in section 4. After this general analysis, we give in section 5 a couple of benchmark examples where either the triboson signals dominate, or have similar size as diboson signals. We summarise our results in section 6.

2 Framework

When considering models that can give a VVX signal corresponding to any of the two topologies in figure 1, we restrict ourselves to particles with spin 0, 1/2 or 1, as those already found in Nature. Furthermore, we consider that $VV = WZ$, since the local significance of the excess with this fat jet selection is larger (3.4σ) than for ZZ (2.9σ) and WW (2.6σ) selections. In order to reproduce the diboson kinematics, the extra particle X should have a mass $m_X = 100 - 200$ GeV, and the secondary resonance Y should have a mass below the TeV.

We will assume that the resonance R decaying into WZX is a charge ± 1 particle and X is a neutral one, because a relatively light charged particle X^\pm would be copiously produced in pairs through its gauge coupling to the photon, leading to a dijet pair signal, so far unobserved [19–22]. If R is a heavy W' boson, it would also explain (see for example refs. [23–25]) a 2.8σ excess in e^+e^-jj production found by the CMS Collaboration [26], at an invariant mass $m_{eejj} \simeq 2$ TeV. On the other hand, for a charged scalar resonance it is harder to justify the required production cross section (see however ref. [27]). These arguments motivate us to extend the SM gauge symmetry with an additional $SU(2)'$.

For the secondary resonance Y , the simplest possibility is to have a new scalar. An additional vector boson, perhaps appearing by enlarging the $SU(2)'$ group, could yield the production and decay topologies in figure 1 too. However, a lighter gauge boson with a mass of few hundreds of GeV, otherwise undetected, should be (almost) fermiophobic, in contrast with the W' boson resonance produced in the s channel. It is unclear that such possibility is viable. Then, we are led to enlarge the scalar sector of the SM. The mixing of the SM scalar sector with additional $SU(2)_L$ singlets or triplets is very constrained by Higgs couplings measurements [28] and precision electroweak data [29], therefore we extend the scalar sector with an additional doublet.

The four complex scalar fields in the two $SU(2)_L$ doublets must transform non-trivially under $SU(2)'$, in order to couple to the W' boson. It seems more natural to arrange them

into two doublets. One possibility is to have a bidoublet, as in LR models; another possibility is that the two $SU(2)_L$ doublets are $SU(2)'$ doublets too. We will restrict ourselves to the first option. Also, some of the quark fields must transform non-trivially under $SU(2)'$, so as to have a W' coupling to quarks. The requirement of gauge invariance of Yukawa terms implies that the $SU(2)'$ doublets must include right-handed quark fields. In the lepton sector, new neutral leptons N_R can be introduced, embedding the right-handed lepton fields into $SU(2)'$ doublets. (Alternatively, the W' boson can be leptophobic if the right-handed as well as the left-handed lepton fields are $SU(2)'$ singlets.) With these assignments, we can identify $SU(2)'$ with a $SU(2)_R$ gauge group.

In this work we will discuss two models, which differ in the way the extended gauge group $SU(2)_L \times SU(2)_R \times U(1)_{B-L}$ is broken to the standard model (SM) one $SU(2)_L \times U(1)_Y$. We consider two distinct scenarios: the triplet [30] and the doublet [31] left-right models (TLRM and DLRM, respectively). In the TLRM, the $SU(2)_R \times U(1)_{B-L}$ breaking occurs through the vacuum expectation value (VEV) of a $SU(2)_R$ triplet

$$\Delta_R = \begin{pmatrix} \Delta_R^+/\sqrt{2} & \Delta_R^{++} \\ \Delta_R^0 & -\Delta_R^+/\sqrt{2} \end{pmatrix} \sim (1, 3, 2), \quad \langle \Delta_R \rangle = \frac{1}{\sqrt{2}} \begin{pmatrix} 0 & 0 \\ v_R & 0 \end{pmatrix}, \quad (1)$$

while in the DLRM, a $SU(2)_R$ doublet χ_R is added instead,

$$\chi_R = \begin{pmatrix} \chi_R^+ \\ \chi_R^0 \end{pmatrix} \sim (1, 2, 1), \quad \langle \chi_R \rangle = \frac{1}{\sqrt{2}} \begin{pmatrix} 0 \\ v_R \end{pmatrix}. \quad (2)$$

Gauge interactions of Δ_R and χ_R are given by the covariant derivatives

$$\begin{aligned} D^\mu \Delta_R &= \partial^\mu \Delta_R - ig_R \left[\frac{\vec{\tau}}{2} \cdot \vec{W}_R^\mu, \Delta_R \right] - ig' B^\mu \Delta_R, \\ D^\mu \chi_R &= \partial^\mu \chi_R - ig_R \frac{\vec{\tau}}{2} \cdot \vec{W}_R^\mu \chi_R - i \frac{g'}{2} B^\mu \chi_R, \end{aligned} \quad (3)$$

where $g_{L,R}$ and g' are gauge coupling constants. The $SU(2)_{L,R}$ and $U(1)_{B-L}$ gauge fields are denoted by $\vec{W}_{L,R}^\mu$, and B^μ , respectively, and $\vec{\tau}$ are the Pauli matrices. Notice that we will not impose any discrete symmetry forcing $g_R = g_L$, as in fully LR symmetric models. The SM gauge group is broken down to $U(1)_{\text{em}}$ by the VEV of a Higgs bidoublet

$$\Phi = \begin{pmatrix} \phi_1^0 & \phi_2^+ \\ \phi_1^- & \phi_2^0 \end{pmatrix} \sim (2, 2, 0), \quad \tilde{\Phi} = \tau_2 \Phi^* \tau_2, \quad (4)$$

to which corresponds the covariant derivative

$$D^\mu \Phi = \partial^\mu \Phi - ig_L \vec{W}_L^\mu \cdot \frac{\vec{\tau}}{2} \Phi + ig_R \Phi \frac{\vec{\tau}}{2} \cdot \vec{W}_R^\mu. \quad (5)$$

The vacuum configuration of Φ is

$$\langle \Phi \rangle = \frac{1}{\sqrt{2}} \begin{pmatrix} v_1 & 0 \\ 0 & e^{i\delta} v_2 \end{pmatrix}, \quad (6)$$

where $v_1 = v \cos \beta$ and $v_2 = v \sin \beta$, with $\tan \beta = v_2/v_1$ and $v = 246$ GeV. In principle, the phase δ could trigger spontaneous CP violation in the scalar sector [32]. Although this is an interesting possibility, for the sake of simplicity of our analysis we set $\delta = 0$.

Gauge boson masses and gauge scalar interactions arise from the gauge-invariant scalar kinetic terms:

$$\begin{aligned} \text{TLRM: } \mathcal{L}_\Phi &= \text{Tr}[(D_\mu \Phi)^\dagger (D^\mu \Phi)] + \text{Tr}[(D_\mu \Delta_R)^\dagger (D^\mu \Delta_R)], \\ \text{DLRM: } \mathcal{L}_\Phi &= \text{Tr}[(D_\mu \Phi)^\dagger (D^\mu \Phi)] + (D_\mu \chi_R)^\dagger D^\mu \chi_R. \end{aligned} \quad (7)$$

The charged gauge boson mass eigenstates are the SM W boson, and a new W' boson, which we identify as being the 2 TeV resonance R in Fig. 1. From eqs. (7) one has, in the limit $v \ll v_R$,

$$M_W \simeq \frac{1}{2} g_L v \left[1 - \frac{\epsilon^2}{2k^2} \sin^2 2\beta \right], \quad M_{W'} \simeq \frac{k}{2} g_R v_R \left[1 + \frac{\epsilon^2}{2k^2} \right], \quad (8)$$

where

$$\epsilon \equiv \frac{v}{v_R} \simeq k \frac{g_R}{g_L} \frac{M_W}{M_{W'}} \ll 1, \quad (9)$$

and $k = \sqrt{2}$ (1) for the TLRM (DLRM). In the above equation, the last inequality stems from $M_{W'} \gg M_W$ and $g_R \sim \mathcal{O}(g_L)$. The mixing between the W and W' mass eigenstates,

$$\begin{pmatrix} W_L^\mu \\ W_R^\mu \end{pmatrix} = \begin{pmatrix} \cos \zeta & -\sin \zeta \\ \sin \zeta & \cos \zeta \end{pmatrix} \begin{pmatrix} W^\mu \\ W'^\mu \end{pmatrix}, \quad (10)$$

is parameterised by an angle ζ for which

$$\tan 2\zeta = \frac{g_L g_R \epsilon^2}{k^2 g_R^2 + (g_R^2 - g_L^2) \epsilon^2} \sin 2\beta \simeq \frac{g_R}{g_L} \frac{M_W^2}{M_{W'}^2} \sin 2\beta \ll 1. \quad (11)$$

Except for $W' \rightarrow WZ$ decays, which are enhanced by $M_{W'}^2/M_W^2$ due to the longitudinal helicity components, we will neglect $W - W'$ mixing, which is equivalent to considering $W^\pm \sim W_L^\pm$ and $W'^\pm \sim W_R^\pm$. The physical neutral gauge bosons Z , Z' and the photon A are related to the weak $\text{SU}(2)_{L,R}$ and $\text{U}(1)_{B-L}$ states $W_L^{3\mu}$, $W_R^{3\mu}$ and B^μ by

$$\begin{pmatrix} W_L^{3\mu} \\ W_R^{3\mu} \\ B^\mu \end{pmatrix} \simeq \begin{pmatrix} c_W & \frac{\epsilon^2}{k^4} \cot \theta_W \cos \varphi \sin^3 \varphi & s_W \\ -s_W \cos \varphi & -\sin \varphi & c_W \cos \varphi \\ -s_W \sin \varphi & \cos \varphi & c_W \sin \varphi \end{pmatrix} \begin{pmatrix} Z^\mu \\ Z'^\mu \\ A^\mu \end{pmatrix}, \quad (12)$$

where $c_W \equiv \cos \theta_W$ and $s_W \equiv \sin \theta_W$, θ_W being the weak mixing angle, and with a new mixing angle φ given by

$$\cos \varphi = \frac{g_L}{g_R} \tan \theta_W, \quad \sin \varphi = \frac{g_L}{g'} \tan \theta_W. \quad (13)$$

The tangent of the $Z - Z'$ mixing angle ξ is given by the ratio of the (1,2) and (1,1) elements of the mixing matrix,

$$\tan \xi = \frac{\cos \varphi \sin^3 \varphi \epsilon^2}{s_W k^4} \ll 1. \quad (14)$$

At zeroth order in the small parameter ϵ , the mixing between the neutral gauge bosons is completely determined by the requirements that (i) the photon couples to the electric charge; and (ii) the Z boson couplings to fermions deviate little from the SM prediction. This also sets a relation among the gauge couplings,

$$g' = \frac{g_L g_R \tan \theta_W}{\sqrt{g_R^2 - g_L^2 \tan^2 \theta_W}}, \quad (15)$$

implying $g_R > g_L \tan \theta_W \simeq 0.55 g_L$. At zeroth order in ϵ , the masses of the neutral gauge bosons Z and Z' are given by

$$M_Z \simeq \frac{g_L v}{2c_W} \simeq \frac{M_W}{c_W}, \quad M_{Z'} \simeq \frac{k^2}{2} v_R \sqrt{g_R^2 + g'^2} \simeq \frac{k}{\sin \varphi} M_{W'}. \quad (16)$$

In both the TLRM and DLRM, the neutral scalar spectrum contains three CP-even scalars h^0 and $H_{1,2}^0$, and one pseudoscalar A^0 . In the limit $v \gg v_R$ (or equivalently $\epsilon \ll 1$), and barring unnatural cancellations, the neutral complex scalar fields $\phi_{1,2}^0$ and Δ_R^0, χ_R^0 can be written in terms of the physical fields as

$$\begin{aligned} \phi_1^0 &\simeq \frac{1}{\sqrt{2}} [-h^0 \sin \alpha + H_1^0 \cos \alpha + i(A^0 \sin \beta + G_1^0 \cos \beta)], \\ \phi_2^0 &\simeq \frac{1}{\sqrt{2}} [h^0 \cos \alpha + H_1^0 \sin \alpha + i(A^0 \cos \beta - G_1^0 \sin \beta)], \\ \Delta_R^0, \chi_R^0 &\simeq \frac{1}{\sqrt{2}} (H_2^0 + G_2^0), \end{aligned} \quad (17)$$

where $G_{1,2}^0$ are the Goldstone bosons and the angle α is the $h_0 - H_1^0$ mixing angle, in the notation of the two Higgs doublet model [33]. Notice that, in general, α depends on the parameters of the scalar potential (see section 5). Moreover, mixing among h_0, H_1^0 and H_2^0 could also occur. However, and since present experimental results seem to indicate that the properties of h^0 are those of the SM Higgs, we will only focus on scenarios which lead to a Higgs mixing pattern like the one given above, with α constrained to lay in the experimentally allowed ranges in the context of a two Higgs doublet model [28].

As for the charged scalar sector, both models include a pair of charged scalars H^\pm , which are related to the components of Φ and Δ_R (or χ_R) by the relations

$$\begin{aligned}\phi_1^\pm &= \frac{kH^\pm \sin \beta}{\sqrt{k^2 + \epsilon^2 \cos^2 2\beta}} + G_1^\pm \cos \beta - \frac{\epsilon G_2^\pm \sin \beta \cos 2\beta}{\sqrt{k^2 + \epsilon^2 \cos^2 2\beta}}, \\ \phi_2^\pm &= \frac{kH^\pm \cos \beta}{\sqrt{k^2 + \epsilon^2 \cos^2 2\beta}} - G_1^\pm \sin \beta - \frac{\epsilon G_2^\pm \cos \beta \cos 2\beta}{\sqrt{k^2 + \epsilon^2 \cos^2 2\beta}}, \\ \Delta_R^\pm, \chi_R^\pm &= \frac{\epsilon H^\pm}{\sqrt{k^2 + \epsilon^2 \cos^2 2\beta}} + \frac{kG_2^\pm}{\sqrt{k^2 + \epsilon^2 \cos^2 2\beta}},\end{aligned}\tag{18}$$

where and $G_{1,2}^\pm$ are the charged Goldstone bosons. In the case of the TLRM, there are two doubly-charged scalars $\Delta_R^{\pm\pm}$ that already are physical. Since we are not interested in the phenomenology related with $\Delta_R^{\pm\pm}$, we consider these states to be heavy enough to not play any significant role in our analysis.

In the approximation of eqs. (17), and taking $\sqrt{k^2 + \epsilon^2 \cos^2 2\beta} \simeq k$ in eqs. (18), the relevant couplings between two vector bosons and one scalar are:

$$\begin{aligned}W^+W^-h^0[H_1^0] &: g_L M_W \sin(\beta - \alpha) [\cos(\beta - \alpha)], \\ W'^\pm W^\mp h^0[H_1^0] &: -g_R M_W \cos(\beta + \alpha) [\sin(\beta + \alpha)], \\ W'^\pm W^\mp A^0 &: \pm i g_R M_W \cos 2\beta, \\ ZZ h^0[H_1^0] &: \frac{g_L M_W}{2c_W^2} \sin(\beta - \alpha) [\cos(\beta - \alpha)], \\ ZZ' h^0[H_1^0] &: \frac{g_R M_W}{c_W} \sin \varphi \sin(\beta - \alpha) [\cos(\beta - \alpha)], \\ W'^\pm Z H^\mp &: -\frac{g_R M_W}{c_W} \cos 2\beta.\end{aligned}\tag{19}$$

Notice that the $W'^\pm Z H^\mp$ interaction receives a contribution from the Δ_R (χ_R) kinetic term. These contributions differ by a $\sqrt{2}$ factor for the triplet and doublet, but the difference is compensated when going to the physical basis, namely eqs. (18). The relevant couplings of one gauge boson to two scalars are

$$\begin{aligned}W^\pm H^\mp h^0[H_1^0] &: \mp \frac{g_L}{2} (p_{h^0[H_1^0]} - p_{H^\pm})^\mu \cos(\beta - \alpha) [-\sin(\beta - \alpha)], \\ W^\pm H^\mp A^0 &: -i \frac{g_L}{2} (p_{A^0} - p_{H^\pm})^\mu, \\ W'^\pm H^\mp h^0[H_1^0] &: \mp \frac{g_R}{2} (p_{h^0[H_1^0]} - p_{H^\pm})^\mu \sin(\beta + \alpha) [-\cos(\beta + \alpha)], \\ W'^\pm H^\mp A^0 &: i \frac{g_R}{2} (p_{A^0} - p_{H^\pm})^\mu \sin 2\beta, \\ ZA^0 h^0[H_1^0] &: -\frac{g_L}{2c_W} (p_{h^0[H_1^0]} - p_{A^0})^\mu \cos(\beta - \alpha) [-\sin(\beta - \alpha)],\end{aligned}$$

$$\begin{aligned}
Z' A^0 h^0 [H_1^0] : & \quad -\frac{g_R}{2} \sin \varphi (p_{h^0 [H_1^0]} - p_{A^0})^\mu \cos(\beta - \alpha) [-\sin(\beta - \alpha)] , \\
Z' H^+ H^- : & \quad \frac{g_R}{2} \sin \varphi (p_{H^+} - p_{H^-})^\mu ,
\end{aligned} \tag{20}$$

with p_X^μ the flowing-in four-momentum of particle X .

In both the TLRM and DLRM, the three lepton and quark families are placed in left- and right-handed doublets

$$\begin{aligned}
Q_{Li} &= \begin{pmatrix} u_i \\ d_i \end{pmatrix}_L \sim (2, 0, 1/3), \quad \ell_{Li} = \begin{pmatrix} \nu_i \\ e_i \end{pmatrix}_L \sim (2, 0, -1), \\
Q_{Ri} &= \begin{pmatrix} u_i \\ d_i \end{pmatrix}_R \sim (0, 2, 1/3), \quad \ell_{Ri} = \begin{pmatrix} \nu_i \\ e_i \end{pmatrix}_R \sim (0, 2, -1),
\end{aligned} \tag{21}$$

where $i = 1, 2, 3$ is a family index. Gauge interactions among fermions and gauge fields are given by:

$$\mathcal{L}_g = \sum_{\psi=Q,\ell} \bar{\psi}_L \gamma^\mu D_\mu^L \psi_L + (L \rightarrow R), \quad D_\mu^{L,R} = i\partial_\mu + g_{L,R} \frac{\vec{\tau}}{2} \cdot \vec{W}_{\mu L, \mu R} + \frac{g'}{2} B^\mu, \tag{22}$$

while the most general Yukawa Lagrangian is:

$$\mathcal{L}_{\text{Yuk}} = -\bar{\ell}_L (Y_\ell \Phi + \tilde{Y}_\ell \tilde{\Phi}) \ell_R - \bar{Q}_L (Y_q \Phi + \tilde{Y}_q \tilde{\Phi}) Q_R + \text{h.c.}, \tag{23}$$

where $Y_{\ell,q}$ and $\tilde{Y}_{\ell,q}$ are general complex Yukawa matrices. In the case of the TLRM, the additional term $-\bar{\ell}_R^c (i\tau_2 \Delta_R) \ell_R$ can be involved in the neutrino mass generation. In general, LRSM models suffer from large flavour-changing neutral current (FCNC) effects due to non-diagonal couplings of the neutral scalars with leptons and quarks. Constraints coming from the analysis of $K_L - K_S$ mass difference require neutral scalar masses larger than 5–10 TeV [34]. This lower bound increases by approximately one order of magnitude if one considers contributions to the CP-violating parameter ϵ_{CP} coming from $\Delta S = 2$ Higgs exchange [35]. Since in our framework we require that H_1^0 , H^\pm and A^0 are relatively light, the Yukawa interactions given above will, in general, lead to unacceptably large FCNC effects. We will therefore consider that the above couplings are somehow suppressed (perhaps due to some extra symmetry) and fermion masses arise from Yukawa interactions generated, for instance, by higher-order operators. Such possibility has been recently explored in Ref. [36], where a Yukawa pattern of the Type II two Higgs doublet model has been reproduced by considering dimension-6 operators of the type $\bar{\psi}_L \tilde{\Phi} \Delta_R^\dagger \Delta_R \psi_R$ and $\bar{\psi}_L \tilde{\Phi} \tilde{\Delta}_R^\dagger \tilde{\Delta}_R \psi_R$, with $\tilde{\Delta}_R = \tau_2 \Delta_R \tau_2$. In the DLRM the same reasoning can be applied replacing Δ_R by the doublet combination $\chi_R \chi_R^\dagger$, which transforms as a triplet under $SU(2)_R$.

3 W' multiboson decays

When kinematically allowed, the W' decay widths into two bosons are

$$\begin{aligned}
\Gamma(W' \rightarrow WZ) &= \frac{g_R^2}{192\pi} \sin^2 2\beta \frac{\lambda(M_{W'}^2, M_W^2, M_Z^2)^{3/2}}{M_{W'}^5} \\
&\quad \times \left(1 + 10 \frac{M_W^2}{M_{W'}^2} + 10 \frac{M_Z^2}{M_{W'}^2} + \frac{M_W^4}{M_{W'}^4} + \frac{M_Z^4}{M_{W'}^4} + 10 \frac{M_W^2 M_Z^2}{M_{W'}^4} \right), \\
\Gamma(W' \rightarrow H^\pm Z) &= \frac{g_R^2}{192\pi c_W^2} \cos^2 2\beta \frac{\lambda(M_{W'}^2, M_Z^2, M_{H^\pm}^2)^{1/2}}{M_{W'}} \\
&\quad \times \left(1 + 10 \frac{M_Z^2}{M_{W'}^2} - 2 \frac{M_{H^\pm}^2}{M_{W'}^2} + \frac{M_Z^4}{M_{W'}^4} + \frac{M_{H^\pm}^4}{M_{W'}^4} - 2 \frac{M_Z^2 M_{H^\pm}^2}{M_{W'}^4} \right), \\
\Gamma(W' \rightarrow WS) &= \frac{g_R^2}{192\pi} x_S^2 \frac{\lambda(M_{W'}^2, M_W^2, M_S^2)^{1/2}}{M_{W'}} \\
&\quad \times \left(1 + 10 \frac{M_W^2}{M_{W'}^2} - 2 \frac{M_S^2}{M_{W'}^2} + \frac{M_W^4}{M_{W'}^4} + \frac{M_S^4}{M_{W'}^4} - 2 \frac{M_W^2 M_S^2}{M_{W'}^4} \right), \\
\Gamma(W' \rightarrow H^\pm S) &= \frac{g_R^2}{192\pi} (1 - x_S^2) \frac{\lambda(M_{W'}^2, M_{H^\pm}^2, M_S^2)^{3/2}}{M_{W'}^5}, \tag{24}
\end{aligned}$$

with $x_S^2 = \cos^2(\beta + \alpha)$, $\sin^2(\beta + \alpha)$, $\cos^2 2\beta$ for $S = h^0, H_1^0, A^0$, respectively, and

$$\lambda(x, y, z) = x^2 + y^2 + z^2 - 2xy - 2xz - 2yz. \tag{25}$$

The partial widths into two fermions are

$$\begin{aligned}
\Gamma(W' \rightarrow f\bar{f}') &= \frac{N_c g_R^2}{48\pi} \frac{\lambda(M_{W'}^2, m_f^2, m_{f'}^2)}{M_{W'}} \\
&\quad \times \left(1 - \frac{m_f^2}{2M_{W'}^2} - \frac{m_{f'}^2}{2M_{W'}^2} - \frac{m_f^4}{2M_{W'}^4} - \frac{m_{f'}^4}{2M_{W'}^4} + \frac{m_f^2 m_{f'}^2}{M_{W'}^4} \right), \tag{26}
\end{aligned}$$

with N_c a colour factor. In the limit that $M_{W'}$ is much larger than the other masses, the branching ratio into two bosons is around 8%.

The scalars S produced in W' decays can further decay into two gauge bosons, a gauge boson plus a lighter scalar, or two fermions. We list here the partial widths, provided the channels are open. For the decay of the heavy neutral scalar they are

$$\begin{aligned}
\Gamma(H_1^0 \rightarrow WW) &= \frac{g_L^2}{64\pi} \cos^2(\beta - \alpha) \frac{M_{H_1^0}^3}{M_W^2} \left(1 - 4 \frac{M_W^2}{M_{H_1^0}^2} \right)^{1/2} \left(1 - 4 \frac{M_W^2}{M_{H_1^0}^2} + 12 \frac{M_W^4}{M_{H_1^0}^4} \right), \\
\Gamma(H_1^0 \rightarrow ZZ) &= \frac{g_L^2}{128\pi c_W^2} \cos^2(\beta - \alpha) \frac{M_{H_1^0}^3}{M_Z^2} \left(1 - 4 \frac{M_Z^2}{M_{H_1^0}^2} \right)^{1/2} \left(1 - 4 \frac{M_Z^2}{M_{H_1^0}^2} + 12 \frac{M_Z^4}{M_{H_1^0}^4} \right),
\end{aligned}$$

$$\begin{aligned}
\Gamma(H_1^0 \rightarrow ZA^0) &= \frac{g_L^2}{64\pi c_W^2} \sin^2(\beta - \alpha) \frac{\lambda(M_{H_1^0}^2, M_Z^2, M_{A^0}^2)^{3/2}}{M_{H_1^0}^3 M_Z^2}, \\
\Gamma(H_1^0 \rightarrow H^+W^-) &= \Gamma(H_1^0 \rightarrow H^-W^+) = \frac{g_L^2}{64\pi} \sin^2(\beta - \alpha) \frac{\lambda(M_{H_1^0}^2, M_W^2, M_{H^\pm}^2)^{3/2}}{M_{H_1^0}^3 M_W^2}, \\
\Gamma(H_1^0 \rightarrow f\bar{f}) &= \frac{N_c h_{ff}^2}{16\pi} M_{H_1^0} \left(1 - 4 \frac{m_f^2}{M_{H_1^0}^2}\right)^{3/2}, \tag{27}
\end{aligned}$$

f being a fermion with Yukawa coupling h_{ff} to H_1^0 . The $H_1^0 h^0 Z$ coupling vanishes and therefore the decay $H_1^0 \rightarrow h^0 Z$ does not take place. The heavy scalar can also decay into $SS = h^0 h^0, A^0 A^0$, with widths

$$\Gamma(H_1^0 \rightarrow SS) = \frac{v^2 \lambda_{H_1^0 SS}^2}{32\pi M_{H_1^0}} \left(1 - 4 \frac{m_S^2}{M_{H_1^0}^2}\right)^{1/2}, \tag{28}$$

with $\lambda_{H_1^0 SS}$ dimensionless trilinear couplings of order unity, which depend on the coefficients in the scalar potential (see section 5) and the mixing in the scalar sector. We will not consider these decays, which are less important for heavier H_1^0 . For the pseudoscalar the widths are

$$\begin{aligned}
\Gamma(A^0 \rightarrow Zh^0) &= \frac{g_L^2}{64\pi c_W^2} \cos^2(\beta - \alpha) \frac{\lambda(M_{A^0}^2, M_Z^2, M_{h^0}^2)^{3/2}}{M_{A^0}^3 M_Z^2}, \\
\Gamma(A^0 \rightarrow ZH_1^0) &= \frac{g_L^2}{64\pi c_W^2} \sin^2(\beta - \alpha) \frac{\lambda(M_{A^0}^2, M_Z^2, M_{H_1^0}^2)^{3/2}}{M_{A^0}^3 M_Z^2}, \\
\Gamma(A^0 \rightarrow H^+W^-) &= \Gamma(A^0 \rightarrow H^-W^+) = \frac{g_L^2}{64\pi} \frac{\lambda(M_{H^\pm}^2, M_W^2, M_{A^0}^2)^{3/2}}{M_{A^0}^3 M_W^2}, \\
\Gamma(A^0 \rightarrow f\bar{f}) &= \frac{N_c (h'_{ff})^2}{16\pi} M_{A^0} \left(1 - 4 \frac{m_f^2}{M_{A^0}^2}\right)^{1/2}, \tag{29}
\end{aligned}$$

with h'_{ff} the Yukawa coupling to A^0 of the fermion f . For the charged scalar,

$$\begin{aligned}
\Gamma(H^\pm \rightarrow Wh^0) &= \frac{g_L^2}{64\pi} \cos^2(\beta - \alpha) \frac{\lambda(M_{H^\pm}^2, M_W^2, M_{h^0}^2)^{3/2}}{M_{H^\pm}^3 M_W^2}, \\
\Gamma(H^\pm \rightarrow WH_1^0) &= \frac{g_L^2}{64\pi} \sin^2(\beta - \alpha) \frac{\lambda(M_{H^\pm}^2, M_W^2, M_{H_1^0}^2)^{3/2}}{M_{H^\pm}^3 M_W^2}, \\
\Gamma(H^\pm \rightarrow WA^0) &= \frac{g_L^2}{64\pi} \frac{\lambda(M_{H^\pm}^2, M_W^2, M_{A^0}^2)^{3/2}}{M_{H^\pm}^3 M_W^2}, \\
\Gamma(H^\pm \rightarrow f\bar{f}') &= \frac{3h_{ff'}^2}{16\pi} \frac{\lambda(M_{H^\pm}^2, m_f^2, m_{f'}^2)}{M_{H^\pm}} \left(1 - \frac{m_f^2}{M_{H^\pm}^2} - \frac{m_{f'}^2}{M_{H^\pm}^2}\right), \tag{30}
\end{aligned}$$

with f, f' two fermions and $h_{ff'}$ their Yukawa coupling to H^\pm . The $H^\pm W^\mp Z$ coupling is absent. We remark that the partial widths into two bosons grow with the third power of

the mass of the decaying scalar, therefore these decays dominate over the rest of decays as soon as there is phase space available. Depending on the scalar mass hierarchy, there is a plethora of possible W' cascade decay chains yielding multiboson signals. We will focus on two simple cases: (i) an alignment scenario where A^0 is lighter than H_1^0 and H^\pm ; (ii) a small misalignment, and the masses of the three new scalars close so that they decay into SM gauge or Higgs bosons. Notice that the constraints on a pseudoscalar [22, 37–39] are very loose, and greatly depend on the couplings assumed to the different fermions. For the charged scalar, we take a mass safely above current limits [40], which anyway depend strongly on the parameters of the model. The same applies to the heavy scalar H_1^0 , which also has suppressed coupling to the W and Z bosons.

3.1 SM-like Higgs scenario

We first consider a scenario where $\beta - \alpha = \pi/2$, in which case h^0 has the properties of the SM Higgs boson, and with A^0 lighter than H_1^0 and H^\pm , assumed to have equal masses for simplicity. We plot in figure 2 the partial widths for the W' decays in eqs. (24), normalised to $g_R = 1$, as a function of β . We take fixed masses $M_{A^0} = 100$ GeV, $M_{H_1^0} = M_{H^\pm} = 500$ GeV. For fixed parameters in the scalar potential, the scalar masses do change with β , therefore figure 2 is intended to illustrate the functional dependence on β of the different decay widths. (The dependence on the H^\pm , H_1^0 and A^0 masses is due to kinematics, and very mild when they are much lighter than $M_{W'}$.)

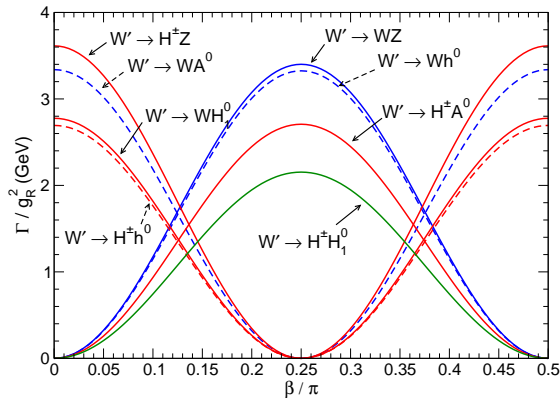


Figure 2: W' partial widths into two bosons for the SM-like Higgs scenario. The blue, red and green lines indicate the modes that, upon decays of H^\pm and H_1^0 , yield dibosons, tribosons and cuadribosons, respectively.

In this scenario, the channels $H_1^0 \rightarrow ZA^0$ and $H^\pm \rightarrow WA^0$ are open and, as aforementioned, these decays are expected to dominate. For example, with the assumed values

for the masses, the Yukawa couplings required to have $\Gamma(H_1^0 \rightarrow b\bar{b}/t\bar{t}) = \Gamma(H_1^0 \rightarrow ZA^0)$ are $h_{bb} = 1.04$, $h_{tt} = 1.66$, respectively, and the coupling required to have $\Gamma(H^\pm \rightarrow t\bar{b}) = \Gamma(H^\pm \rightarrow WA^0)$ is $h_{tb} = 1.2$. We therefore neglect the decays of H_1^0 and H^\pm into quarks, while A^0 is expected to decay into $b\bar{b}$. We collect in table 1 the multiboson signals produced in W' cascade decays, for the scenario here considered. We present in figure 3 (left)

dibosons	tribosons	quadribosons
$W' \rightarrow WZ$	$W' \rightarrow H^\pm Z \rightarrow WA^0 Z$	$W' \rightarrow H^\pm H_1^0 \rightarrow WA^0 ZA^0$
$W' \rightarrow Wh^0$	$W' \rightarrow WH_1^0 \rightarrow WZA^0$	
$W' \rightarrow WA^0$	$W' \rightarrow H^\pm h^0 \rightarrow WA^0 h^0$	
	$W' \rightarrow H^\pm A^0 \rightarrow WA^0 A^0$	

Table 1: Multiboson signals from W' decays in an alignment scenario with A^0 lighter than H_1^0 and H^\pm .

the total size of the WZ diboson (blue) and WZX triboson (red) signals as a function of β . On the right panel we do the same for the Wh^0 and $Wh^0 X$ signals. Additionally, we include the partial widths to WA^0 and $WA^0 X$. These final states could mimick the ones with a Higgs boson if $M_{A^0} \sim M_{h^0}$, as the mass window typically used for tagging fat jets as h^0 candidates is wide, for example $110 \leq m_J \leq 135$ GeV in ref. [7].

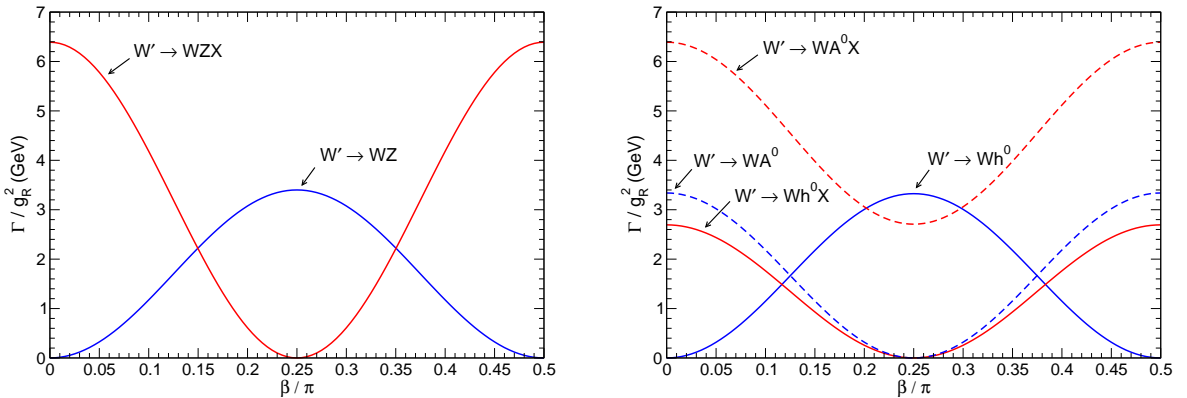


Figure 3: Left: W' partial widths into WZ (dibosons) and WZX (tribosons), with $X = A^0$. Right: W' partial widths into Wh^0 , WA^0 (dibosons) and $Wh^0 X$, $WA^0 X$ (tribosons).

3.2 Higgs mixing scenario

Current limits on Higgs couplings [28] allow for small deviations from the SM prediction, in particular a small non-zero $\cos(\beta - \alpha)$. We parameterise these deviations introducing a small angle γ so that $\beta - \alpha = \pi/2 - \gamma$. We consider a scenario where H_1^0 , H^\pm and A^0 have similar masses so that decays among them are kinematically forbidden (for sufficiently large mass splittings, decays with off-shell W/Z bosons may be important). For simplicity, we take all their masses equal, $M_{H_1^0} = M_{A^0} = M_{H^\pm} = 500$ GeV. The dependence on the angle β of the W' decay widths into two bosons, normalised to $g_R = 1$, is plotted in figure 4, taking a small misalignment $\sin \gamma = 0.1$. Notice that there is a small phase shift $\gamma/2$ with respect to figure 2 in the partial widths for $W' \rightarrow Wh^0$, $W' \rightarrow WH_1^0$, $W' \rightarrow H^\pm h^0$, and $W' \rightarrow H^\pm H_1^0$.

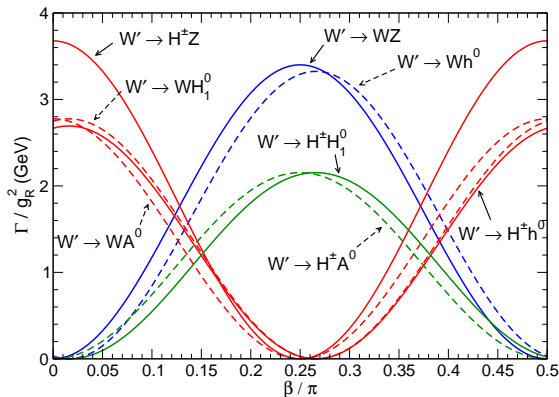


Figure 4: W' partial widths into two bosons for the Higgs mixing scenario. The blue, red and green lines indicate the modes that, upon decays of H^\pm , A^0 and H_1^0 , yield dibosons, tribosons and cuadribosons, respectively.

The small mixing $\cos(\beta - \alpha) = \sin \gamma$ allows decays into SM gauge or Higgs bosons, i.e. $H_1^0 \rightarrow W^+W^-$, $H_1^0 \rightarrow ZZ$, $A^0 \rightarrow Zh^0$, $H^\pm \rightarrow Wh^0$, although they compete with the decays into fermions. We classify in table 2 the possible multiboson signals from W' cascade decays. In figure 5 (left) the total size of the WZ diboson (blue), WZX (red) and WWX (orange) triboson signals is plotted as a function of β . For triboson signals, the solid lines correspond to negligible Yukawa couplings. For the dashed lines, we have chosen $h_{bb} = h'_{bb}$, equal to the SM bottom quark Yukawa coupling; $h_{tt} = h'_{tt}$, equal to the SM top quark Yukawa coupling; and $h_{tb} = \sqrt{h_{bb}h_{tt}}$. On the right panel we present the Wh^0 and Wh^0X signals.

dibosons	tribosons	quadribosons
$W' \rightarrow WZ$	$W' \rightarrow WH_1^0 \rightarrow WWW$	$W' \rightarrow H^\pm H_1^0 \rightarrow Wh^0 WW$
$W' \rightarrow Wh^0$	$W' \rightarrow WH_1^0 \rightarrow WZZ$	$W' \rightarrow H^\pm H_1^0 \rightarrow Wh^0 ZZ$
	$W' \rightarrow WA^0 \rightarrow WZh^0$	$W' \rightarrow H^\pm A^0 \rightarrow Wh^0 Zh^0$
	$W' \rightarrow H^\pm Z \rightarrow Wh^0 Z$	
	$W' \rightarrow H^\pm h^0 \rightarrow Wh^0 h^0$	

Table 2: Multiboson signals from W' decays in the Higgs mixing scenario with H_1^0 , A^0 and H^\pm of similar mass, and non-zero $\cos(\beta - \alpha)$.

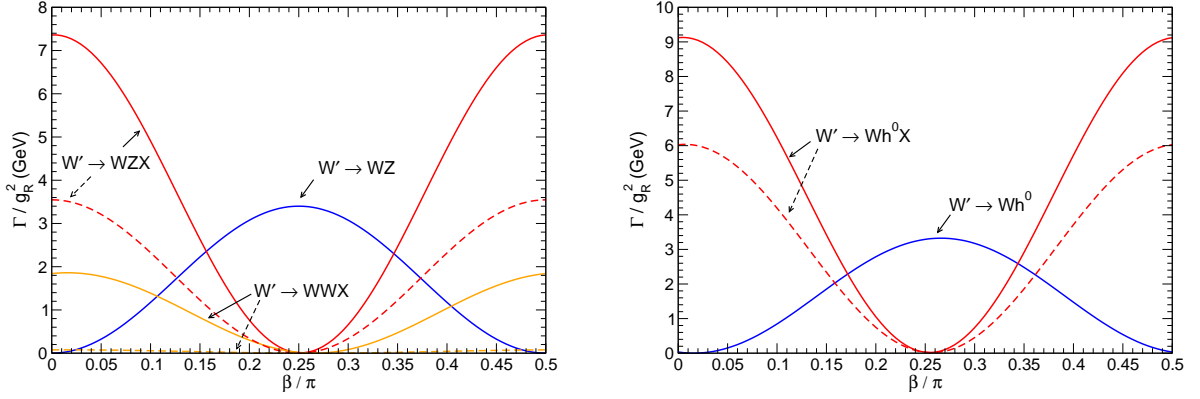


Figure 5: Left: W' partial widths into WZ (dibosons) and WZX , WWX (tribosons). Right: W' partial widths into Wh^0 (dibosons) and Wh^0X (tribosons). For triboson signals, the solid line corresponds to negligible Yukawa couplings and the dashed lines to the assumption given in the text.

4 Multiboson cross sections

So far we have considered the relative size of diboson and triboson signals in two simplified scenarios, and their dependence on the angle β . We now address the possible size of these signals for a W' boson with a mass near 2 TeV. The next-to-leading order W' cross section [41] at a centre-of-mass (CM) energy of 8 TeV can be parameterised as

$$\sigma_{W'}(\text{pb}) = 638 g_R^2 \times \exp[-4.02M - 0.088M^2 - 0.073M^3], \quad (31)$$

with M the W' mass in TeV. The total W' width is nearly independent of β , $\Gamma = 167 g_R^2$ GeV in the alignment scenario and $\Gamma = 166.5 g_R^2$ GeV in the Higgs mixing scenario, with a negligible variation of ± 0.5 GeV depending on β . The approximate WZ diboson and WZX/WWX triboson branching ratios are collected in table 3. In both cases we include the decays of the W' boson into the three generations of light leptons plus a heavy neutrino

	$\text{Br}(W' \rightarrow WZ)$	$\text{Br}(W' \rightarrow WZX)$	$\text{Br}(W' \rightarrow WWX)$
alignment	$0.02 \sin^2 2\beta$	$0.039 \cos^2 2\beta$	0
mixing	$0.02 \sin^2 2\beta$	$0.044 \cos^2 2\beta$	$0.011 \cos^2 2\beta$

Table 3: Diboson and triboson branching ratios for the Higgs alignment and Higgs mixing scenarios.

N , with a mass taken as 500 GeV. Notice that in the Higgs mixing scenario the triboson signals may be depleted by the H_1^0 , A^0 , H^\pm decays into fermions. The maximum size of diboson plus triboson signals depends on the relative efficiencies of each one, which can only be obtained with a detailed simulation, out of the scope of this work.

The possible size of the coupling g_R is constrained by other processes. Searches for $W' \rightarrow t\bar{b}$ production by the CMS Collaboration yield a limit $\sigma(W' \rightarrow t\bar{b}) \leq 40$ fb with a 95% confidence level (CL) [42] for W' masses between 1.9 and 2.2 TeV, where a sum of $t\bar{b}$ and $\bar{t}b$ final states is understood. Limits from the ATLAS Collaboration [43,44] are looser. In a flavour-diagonal scenario (with no W' charged mixing), and independently of the presence of other decay channels, $\Gamma(W' \rightarrow WZ)/\Gamma(W' \rightarrow t\bar{b}) \sim \sin^2 2\beta/12$, therefore one has a maximum $\sigma(W' \rightarrow WZ) = 3.3$ fb, only one half of the cross section needed to explain the number of excess events at the 2 TeV peak [8]. Analogously, $\sigma(W' \rightarrow WZX + WWX)$ has a maximum of 6 – 9 fb, also below the required cross section especially since the efficiency is smaller than for WZ . However, the constraint from $W' \rightarrow t\bar{b}$ can be softened or even evaded if a nearly diagonal W' quark mixing matrix is not assumed.

Another constraint results from dijet production. The ATLAS Collaboration sets a limit [45] $\sigma(W' \rightarrow jj) \times \mathcal{A} \leq 60$ fb for $M_{W'} = 2$ TeV, with a 95% CL. With an acceptance $\mathcal{A} \simeq 0.45$ [45], this constraint is translated into $\sigma(W') \leq 280$ fb, i.e. $g_R \leq 1.05$, if all decay channels are open. The CMS Collaboration sets a similar limit [46], $\sigma(W' \rightarrow jj) \times \mathcal{A} \leq 100$ fb for $M_{W'} = 2$ TeV. Taking an approximate acceptance of 0.64 [46] (for isotropic decays) yields a looser limit, $\sigma(W') \leq 330$ fb. Interestingly, the CMS Collaboration observes a 2σ excess but at slightly smaller invariant masses, $m_{jj} \simeq 1.8$ TeV.

A third constraint results from the non-observation of the heavy Z' boson. The relation between the W' and Z' masses depends on the representation of the scalars that break $\text{SU}(2)_R$, and also on the coupling g_R . We plot in figure 6 (left) the ratio $M_{Z'}/M_{W'}$ as a function of g_R/g_L in the two cases that $\text{SU}(2)_R$ is broken by a scalar doublet and a scalar triplet. On the right panel we plot the $Z' \rightarrow e^+e^-$ branching ratio, as well as the branching ratio for the Z' bosonic decay modes, as a function of g_R/g_L . The Z' boson is taken much heavier than its decay products.

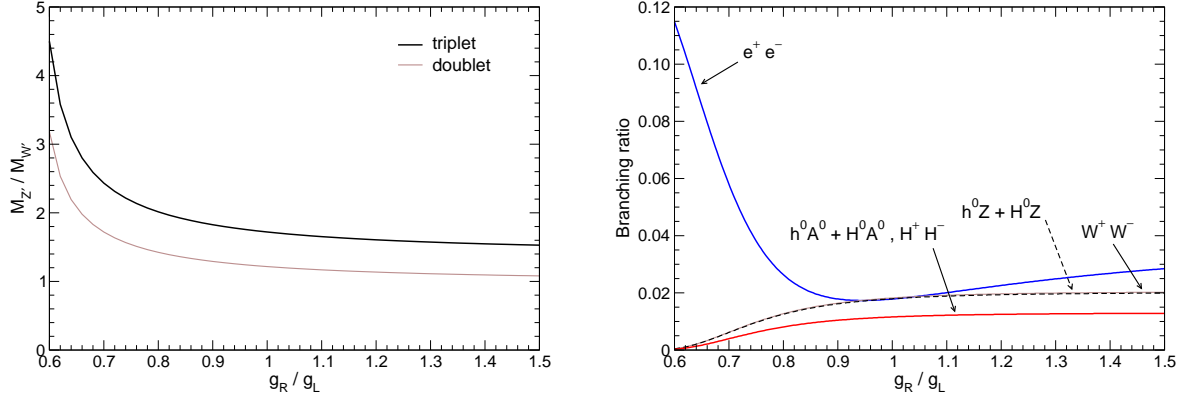


Figure 6: Left: $M_{Z'}/M_{W'}$ ratio as a function of g_R/g_L . Right: Z' branching ratio to e^+e^- and bosonic modes, as a function of g_R/g_L

Combining the cross section dependence on the mass and couplings, and the coupling dependence of the Z' boson mass, we plot in figure 7 the total Z' boson production cross section at leading order, as a function of g_R/g_L , as well as the $Z' \rightarrow e^+e^-$ cross section, for a reference W' mass of 2 TeV and CM energies of 8 TeV and 13 TeV. A K factor of 1.16 [47] is included to approximately reproduce the NLO cross section [48]. For Z' masses of 2–3 TeV, the unobservation of a signal in the 8 TeV run by the ATLAS Collaboration [47] implies $\sigma(Z' \rightarrow e^+e^-) \lesssim 0.2$ fb, assuming lepton universality. Therefore, for a fixed W' mass of 2 TeV, Z' boson searches imply $g_R/g_L \leq 1$ for the doublet, while they do not constrain the range of g_R shown in the case of the triplet. For heavier W' bosons, the limits are looser.

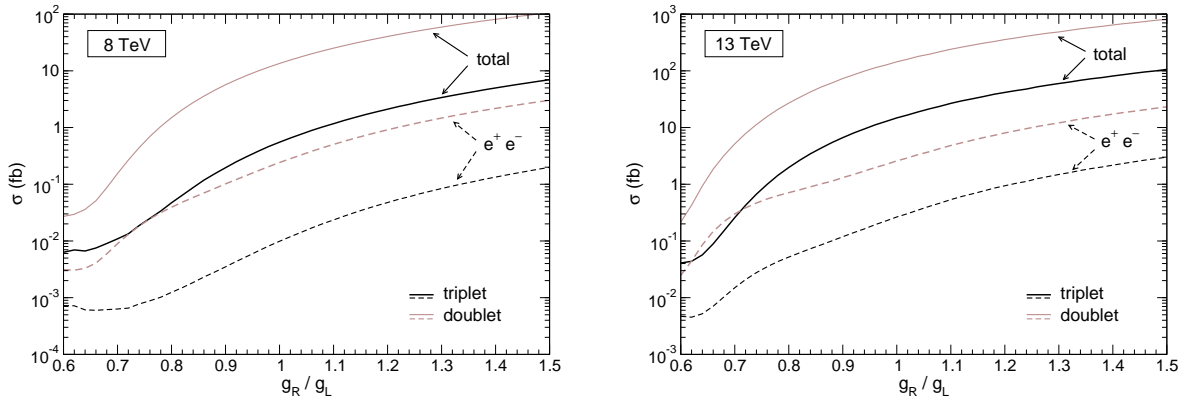


Figure 7: Total Z' production cross section and $Z' \rightarrow e^+e^-$ cross section as a function of g_R/g_L , assuming a fixed W' mass of 2 TeV, for CM energies of 8 TeV (left) and 13 TeV (right).

We conclude this section by discussing possible low-energy and precision electroweak data constraints on the W' and Z' masses and mixings [49–51]. In the specific context of LR symmetric models, limits on $M_{W'}$, $M_{Z'}$ and their corresponding mixing angles have been obtained, for instance, in Refs. [52–55]. For a small $W - W'$ mixing angle ζ we have, from eq. (11) and taking $M_{W'} = 2$ TeV,

$$\zeta_g \equiv \frac{g_R}{g_L} \zeta \simeq \frac{1}{2} \frac{g_R^2}{g_L^2} \frac{M_W^2}{M_{W'}^2} \sin 2\beta \simeq 0.0008 \frac{g_R^2}{g_L^2} \sin 2\beta. \quad (32)$$

For g_R of order unity, ζ_g is below the upper limits in ref. [52], which are of the order $|\zeta_g| \lesssim (1-2) \times 10^{-3}$, depending on the assumptions about the mixing in the right-handed sector. For the same W' mass, the $Z - Z'$ mixing angle is

$$\xi \simeq \frac{0.0016 (g_R^2 - g_L^2 \tan^2 \theta_W)^{3/2}}{k^2 g_L g_R^2 c_W}, \quad (33)$$

with $k^2 = 2$ (1) for the TLRM (DLRM). The second factor in the above equation is of order unity, *e. g.* it is approximately 1.5 for $g_R = 1$, therefore the neutral mixing is compatible with the constraints from low-energy and LEP data, $-0.00040 < \xi < 0.0026$ [54]. A similar analysis presented in ref. [55] shows that, for $M_{W'} = 2$ TeV, $M_{Z'}/M_{W'} \gtrsim 1.6$ (1.2) for the TLRM (DLRM). According to figure 6, this implies $g_R/g_L \lesssim 1.2$ (1.0). Although these bounds are slightly in tension with the cases we are interested in, they can be relaxed with the addition of extra matter content, which naturally appears in embeddings of the $SU(2)_L \times SU(2)_R$ in a larger group.²

5 Benchmark examples

In this section we analyse benchmark scenarios that can account for multiboson production in the context of the TLRM and DLRM, providing some examples of the general behaviour discussed in section 3. This requires specifying the scalar potential V , which can be written as

$$V = V_\Phi + V_{\Phi_R} + V_{\Phi_R, \Phi}, \quad (34)$$

where V_Φ and V_{Φ_R} contain only terms with Φ and $\Phi_R \equiv \Delta_R$ (χ_R) in the DLRM (TLRM), respectively, and mixed terms involving both Φ and Φ_R are included in $V_{\Phi_R, \Phi}$. The most

²According to ref. [55], the measurements that mainly drive the limits for this model are the b -quark forward-backward asymmetry at LEP and the Z boson hadronic width. These two quantities are also modified when vector-like fermions mix with the third generation [56].

general gauge invariant scalar potential V_Φ is [57]

$$V_\Phi = -\mu_1^2 \text{Tr}(\Phi^\dagger\Phi) - \mu_2^2 \left[\text{Tr}(\tilde{\Phi}\Phi^\dagger) + \text{Tr}(\tilde{\Phi}^\dagger\Phi) \right] + \lambda_1 \text{Tr}(\Phi^\dagger\Phi)^2 + \lambda_2 \left[\text{Tr}(\tilde{\Phi}\Phi^\dagger)^2 + \text{Tr}(\tilde{\Phi}^\dagger\Phi)^2 \right] + \lambda_3 \text{Tr}(\tilde{\Phi}\Phi^\dagger) \text{Tr}(\tilde{\Phi}^\dagger\Phi) + \lambda_4 \text{Tr}(\Phi^\dagger\Phi) \left[\text{Tr}(\tilde{\Phi}\Phi^\dagger) + \text{Tr}(\tilde{\Phi}^\dagger\Phi) \right], \quad (35)$$

where μ_i are mass parameters, and λ_i are dimensionless. (For simplicity we restrict ourselves to the case of real coefficients in the potential.) The pure Φ_R terms for the TLRM (DLRM) are

$$\begin{aligned} V_{\Delta_R} &= -\mu_3^2 \text{Tr}(\Delta_R^\dagger\Delta_R) + \alpha_1 \text{Tr}(\Delta_R^\dagger\Delta_R)^2 + \alpha_2 \text{Tr}(\Delta_R\Delta_R) \text{Tr}(\Delta_R^\dagger\Delta_R^\dagger), \\ V_{\chi_R} &= -\mu_3^2 \chi_R^\dagger\chi_R + \alpha_1(\chi_R^\dagger\chi_R)^2, \end{aligned} \quad (36)$$

while for the mixed terms $V_{\Phi_R,\Phi}$ one has

$$\begin{aligned} V_{\Delta_R,\Phi} &= \rho_1 \text{Tr}(\Phi^\dagger\Phi) \text{Tr}(\Delta_R^\dagger\Delta_R) + \rho_2 \text{Tr}(\Phi^\dagger\Phi\Delta_R\Delta_R^\dagger) \\ &\quad + \rho_3 \left[\text{Tr}(\Phi\tilde{\Phi}^\dagger) + \text{Tr}(\Phi^\dagger\tilde{\Phi}) \right] \text{Tr}(\Delta_R^\dagger\Delta_R), \\ V_{\chi_R,\Phi} &= \rho_1 \text{Tr}(\Phi^\dagger\Phi)\chi_R^\dagger\chi_R + \rho_2 \chi_R^\dagger\Phi^\dagger\Phi\chi_R + \rho_3 \chi_R^\dagger(\tilde{\Phi}^\dagger\Phi + \Phi^\dagger\tilde{\Phi})\chi_R. \end{aligned} \quad (37)$$

Notice that, in general, other invariant dimension-4 combinations of the fields can be included in V . However, it can be shown that those can always be written as linear combinations of the terms given above. Detailed analyses of the above potential have been presented in refs. [31,57,58]. Here, in order to provide representative examples of the benchmark scenarios discussed in section 3, it is sufficient to consider simpler cases where some of the parameters in the potential vanish. In the first one, labeled as benchmark A, we impose a discrete symmetry $\Phi \rightarrow i\Phi$ to the scalar potential, and set $v_2 = 0$ [31,58]. This corresponds to having $\mu_2^2 = 0$ in eq. (35) and $\rho_3 = 0$ in eqs. (37). In the second one, labeled as benchmark B, we set $\lambda_4 = \rho_1 = \rho_3 = 0$ which, although not motivated by any special symmetry, will allow us to reproduce analytically the Higgs-mixing scenario considered in section 3.

In benchmark A the minimisation conditions $\partial V/\partial v_{1,R} = 0$ allow to write the mass parameters $\mu_{1,3}^2$ as

$$\mu_1^2 = \lambda_1 v^2 + \frac{\rho_1}{2} v_R^2, \quad \mu_3^2 = \alpha_1 v_R^2 + \frac{\rho_1}{2} v^2. \quad (38)$$

Notice that in this case $v_1 = v$ since $v_2 = 0$. Inserting the above equalities in V , one can obtain the neutral scalar masses,

$$\begin{aligned} m_{h^0}^2 &\simeq \frac{4\alpha_1\lambda_1 - \rho_1^2}{2\alpha_1} v^2, & m_{H_1^0}^2 &\simeq 2v^2(2\lambda_2 + \lambda_3) + \frac{\rho_2}{2} v_R^2, \\ m_{H_2^0}^2 &\simeq 2\alpha_1 v_R^2 + \frac{\rho_1^2}{2\alpha_1} v^2, & m_{A^0}^2 &= \frac{\rho_2}{2} v_R^2 + 2v^2(\lambda_3 - 2\lambda_2), \end{aligned} \quad (39)$$

as well as the charged scalar mass,

$$m_{H^\pm}^2 = \frac{\rho_2}{2k^2} (k^2 v_R^2 + v^2), \quad (40)$$

where, as before, $k = \sqrt{2}(1)$ for the TLRM (DLRM). From these expressions we conclude that ρ_2 has to be positive and small in order to yield $m_{H^\pm} \ll v_R$. Also, since we are taking $m_{H_2^0}^2 \sim v_R$, we must have $\alpha_1 > 0$. This implies $4\alpha_1\lambda_1 > \rho_1^2$ to have a positive $m_{h^0}^2$. Inverting these equations, we can obtain approximate expressions for the potential parameters in terms of the scalar masses,

$$\begin{aligned} \lambda_1 &\simeq \frac{1}{4v^2} \left(m_{H_1^0}^2 + 2m_{h^0}^2 - \sqrt{m_{H_1^0}^4 - 4v_R^2 v^2 \rho_1^2} \right), \quad \lambda_2 \simeq \frac{m_{H_1^0}^2 - m_{A^0}^2}{8v^2}, \\ \lambda_3 &\simeq \frac{1}{4v^2} \left(m_{A^0}^2 + m_{H_1^0}^2 - 2m_{H^\pm}^2 \right), \quad \alpha_1 \simeq \frac{1}{4v^2} \left(m_{H_1^0}^2 + \sqrt{m_{H_1^0}^4 - 4v_R^2 v^2 \rho_1^2} \right), \\ \rho_2 &\simeq \frac{2m_{H^\pm}^2}{v_R^2}. \end{aligned} \quad (41)$$

Choosing a scalar spectrum similar to that considered in the previous section,

$$m_{h^0} = 125 \text{ GeV}, \quad m_{H_1^0} = m_{H^\pm} = 500 \text{ GeV}, \quad m_{A^0} = 100 \text{ GeV}, \quad m_{H_2^0} = 4 \text{ TeV}, \quad (42)$$

and taking $M_{W'} = 2 \text{ TeV}$ and $g_R = 1$, we get for the TLRM and DLRM the parameters

$$\begin{aligned} \text{TLRM: } &\lambda_1 \simeq 0.38, \quad \lambda_2 \simeq 0.50, \quad \lambda_3 \simeq -0.98, \quad \alpha_1 \simeq 1.0, \quad \rho_2 \simeq 0.06, \\ \text{DLRM: } &\lambda_1 \simeq 0.63, \quad \lambda_2 \simeq 0.50, \quad \lambda_3 \simeq -0.98, \quad \alpha_1 \simeq 0.50, \quad \rho_2 \simeq 0.03, \end{aligned} \quad (43)$$

for $\rho_1 = 1$. At first order in ϵ the neutral complex scalar fields $\phi_{1,2}^0$ and χ_R^0, Δ_R^0 can be written as

$$\begin{aligned} \phi_1^0 &\simeq \frac{-h^0 + s_{13}H_2^0 + iG_1^0}{\sqrt{2}}, \quad \phi_2^0 \simeq \frac{H_1^0 + iA^0}{\sqrt{2}}, \\ \Delta_R^0, \chi_R^0 &\simeq \frac{s_{13}h_0 + H_2^0 + iG_2^0}{\sqrt{2}}, \end{aligned} \quad (44)$$

with

$$s_{13} \simeq \frac{\epsilon \rho_1}{2\alpha_1} \simeq \frac{2\epsilon\rho_1 v_R^2}{m_{H_1^0}^2 + \sqrt{m_{H_1^0}^4 - 4v_R^2 v^2 \rho_1^2}}. \quad (45)$$

When compared with eqs. (17), this leads to $\cos(\beta - \alpha) = \cos \alpha = 0$, i.e. no Higgs mixing. Notice that the mixing with H_2^0 (parameterised by s_{13}) is always small, even if $\rho_1 \sim 1$. Besides, in this benchmark the trilinear couplings $\lambda_{H_1^0 h^0 h^0}$ and $\lambda_{H_1^0 A^0 A^0}$ identically vanish.

In benchmark B, for which $\lambda_4 = \rho_1 = \rho_3 = 0$, the minimisation conditions with respect to $v_{1,2}$ and v_R lead to

$$\begin{aligned}\mu_1^2 &= \lambda_1 v^2 - \frac{\rho_2 v_R^2 \sin^2 \beta}{2 \cos 2\beta}, \\ \mu_2^2 &= \left(\lambda_2 + \frac{\lambda_3}{2} \right) v^2 \sin 2\beta + \frac{\rho_2}{8} v_R^2 \tan 2\beta, \\ \mu_3^2 &= \frac{\rho_2}{2} v^2 \sin 2\beta + \alpha_1 v_R^2.\end{aligned}\tag{46}$$

The masses of the CP-even and CP-odd scalars are in this case

$$\begin{aligned}m_{h^0}^2 &\simeq 2 [\lambda_1 + (2\lambda_2 + \lambda_3) \sin^2 2\beta] v^2, \\ m_{H_1^0}^2 &\simeq \frac{\rho_2 v_R^2}{2 \cos 2\beta} + 2v^2 (2\lambda_2 + \lambda_3) \cos^2 2\beta, \\ m_{H_2^0}^2 &\simeq \frac{v_R^2}{2\alpha_1} (4\alpha_1^2 + \epsilon^2 \rho_2^2 \sin^4 \beta), \\ m_{A^0}^2 &= \frac{\rho_2 v_R^2}{2 \cos 2\beta} + 2v^2 (\lambda_3 - 2\lambda_2),\end{aligned}\tag{47}$$

where the dependence on the angle β is apparent. The charged scalar mass is

$$m_{H^\pm}^2 = \frac{\rho_2}{2k^2 \cos 2\beta} [k^2 v_R^2 + v^2 \cos^2 2\beta].\tag{48}$$

Again, inverting these equations we can find the potential parameters in terms of the scalar masses,

$$\begin{aligned}\lambda_1 &\simeq \frac{1}{2v^2} [m_{h^0}^2 + (m_{H^\pm}^2 - m_{H_1^0}^2) \tan^2 2\beta], \\ \lambda_2 &\simeq \frac{1}{8v^2 \cos^2 2\beta} [m_{H_1^0}^2 - m_{H^\pm}^2 + (m_{H^\pm}^2 - m_{A^0}^2) \cos^2 2\beta], \\ \lambda_3 &\simeq \frac{1}{4v^2 \cos^2 2\beta} [m_{H_1^0}^2 - m_{H^\pm}^2 - (m_{H^\pm}^2 - m_{A^0}^2) \cos^2 2\beta], \\ \alpha_1 &\simeq \frac{m_{H_2^0}^2}{2v_R^2}, \quad \rho_2 \simeq \frac{2m_{H^\pm}^2 \cos 2\beta}{v_R^2}.\end{aligned}\tag{49}$$

In contrast with benchmark A, here the Higgs mixing pattern is non-trivial. In particular, the alignment condition $\cos(\beta - \alpha) = 0$ is not automatically fulfilled since

$$\cos(\beta - \alpha) \simeq \frac{4\epsilon^2}{\rho_2} (2\lambda_2 + \lambda_3) \cos^2 2\beta \simeq \frac{\Delta m_H^2 + \epsilon^2 m_{H_1^0}^2 \cos^2 2\beta}{m_{H^\pm}^2} \tan 2\beta,\tag{50}$$

which is still very small if $\Delta m_H^2 \equiv m_{H_1^0}^2 - m_{H^\pm}^2 = 0$. However, by slightly lifting the degeneracy assumption between the H_1^0 and H^\pm masses, one can in principle obtain a

sizable $h^0 - H_1^0$ mixing. Besides, mixing in the 1 – 3 and 2 – 3 CP-even neutral scalar sectors will be also generated³,

$$\theta_{13} \simeq \frac{m_{H^\pm}^4 \epsilon \sin \beta \sin(4\beta)}{2m_{H_2^0}^2(m_{H^\pm}^2 - m_{H_2^0}^2)}, \quad \theta_{23} \simeq \frac{\epsilon m_{H^\pm}^2 (m_{H_2^0}^2 - m_{H^\pm}^2 \sin^2 \beta) \cos(2\beta) \sin \beta}{m_{H_2^0}^2 (m_{H_2^0}^2 - m_{H^\pm}^2)}, \quad (51)$$

but it is always very small because $\epsilon \ll 1$ and $m_{H^\pm}/m_{H_2} \ll 1$.

As numerical example we take $\cos(\beta - \alpha) \simeq 0.1$ with $\beta = 0.1\pi$, in which case W' decays yield diboson plus triboson production. The spectrum is the same as in (42), except for the charged-Higgs mass that we now take as $m_{H^\pm} = 530$ GeV, in order to obtain a non-zero Higgs mixing. This spectrum results from the scalar parameters

$$\begin{aligned} \text{TLRM} : \quad & \lambda_1 \simeq 0.24, \quad \lambda_2 \simeq 0.47, \quad \lambda_3 \simeq -1.3, \quad \alpha_1 \simeq 1.0, \quad \rho_2 \simeq 0.06, \\ \text{DLRM} : \quad & \lambda_1 \simeq 0.24, \quad \lambda_2 \simeq 0.47, \quad \lambda_3 \simeq -1.3, \quad \alpha_1 \simeq 0.50, \quad \rho_2 \simeq 0.03. \end{aligned} \quad (52)$$

We note that in this benchmark we cannot obtain mixing $\cos(\beta - \alpha) \neq 0$ for $\beta = 0$, as it can be observed from eq. (50).

6 Discussion

The ATLAS excess [1] in JJ production near $m_{JJ} = 2$ TeV is kinematically compatible with the production of a heavy resonance decaying into two bosons W/Z plus an extra particle X , with an intermediate resonance as in figure 1. As a possible realisation of this mechanism, in this paper we have considered a SM extension with an additional $SU(2)_R$, in which the new gauge boson W' is the natural candidate to explain the JJ excess. We have shown in two simple scenarios that, provided the additional scalars present in the model are lighter than the W' boson, the decays $W' \rightarrow WZX$ can dominate over decays $W' \rightarrow WZ$, as their respective partial widths are proportional to $\cos^2 2\beta$ and $\sin^2 2\beta$. In case there is a strong hierarchy among the VEVs of the two neutral scalars that break the $SU(2)_L$ gauge symmetry, $W' \rightarrow WZ$ decays will be largely suppressed ($\sin 2\beta \sim 0$) with the rate for $W' \rightarrow WZX$ reaching its apex ($\cos 2\beta \sim 1$). If such a hierarchy does not exist, we will have a mixture of WZ and WZX production in general, unless the two VEVs are equal, in which case WZX production is suppressed. The latter is the situation considered in previous literature [9] explaining the excess as $W' \rightarrow WZ$ production.

Besides the kinematics, one has to consider the size itself of the observed excess. For a $SU(2)_R$ coupling $g_R = 1$ and $\cos 2\beta = 1$, the triboson cross section is $\sigma_{WZX} \gtrsim 10$ fb. (For

³Here, θ_{13} and θ_{23} are defined according to the standard parameterisation of a unitary 3×3 matrix [40].

comparison, the maximum diboson signal is one half of this value for the same g_R .) While in principle this cross section is of the magnitude needed to explain the excess in ref. [1], the efficiency for triboson signals is expected to be smaller [8]. A careful evaluation of this efficiency — which depends not only on the precise details of the boson tagging but also on the identity of the particle X and its mass — is out of the scope of this work. In the absence of such a detailed simulation, several qualitative arguments suggest that the efficiency for triboson signals may be not too low so as to explain the ATLAS diboson excess.

1. The decrease in selection efficiency would be around a factor of six [8] if only the kinematical configurations where the extra particle X is well separated from the W and Z bosons were to contribute to a “diboson” signal after the kinematical selection requirements of the ATLAS analysis [1]. However, it is expected that configurations where X (or some of its decay products) merge with the bosons will also contribute to this signal.
2. In this respect, one of the boson tagging variables used by the ATLAS Collaboration is the jet mass m_J , which is required to lie in a suitable interval around the W or Z pole mass. Clearly, if X merges with a boosted W/Z boson, then m_J will increase, thus reducing the boson tagging efficiency compared to the direct $W' \rightarrow WZ$ decay. Another tagging variable is the number of tracks N_{trk} in the jet, required to be $N_{\text{trk}} \leq 30$ [1,11]. Likewise, if X merges with a boosted W/Z boson, the number of tracks in the jet will be larger and the boson tagging efficiency will be correspondingly lower. As a consequence of these tagging requirements, for the kinematical configurations where X merges with the W/Z bosons one expects a reduced, but not zero, boson tagging efficiency.
3. In the run 2 JJ search [11], the ATLAS Collaboration has provided results for the JJ invariant mass distribution when requirements on one of these boson tagging variables are dropped. Interestingly, when the m_J or N_{trk} cuts are not applied, slight bumps in the m_{JJ} distributions are seen around $m_{JJ} = 2$ TeV, which are not visible when the full boson tagging is performed. Although the dataset is still limited by statistics and definite conclusions cannot be drawn, this feature certainly deserves a more detailed investigation.
4. Additional processes may mimic WZ or WZX production, for example WA^0 , WA^0A^0 and WA^0h^0 production, if the new pseudoscalar A^0 has a mass similar to the W/Z masses, thus also increasing the potential signal.

On the other hand, the possibility that g_R is larger than unity is in principle allowed, leading to larger triboson cross sections. In this respect, the W' gauge couplings to the quarks can be reduced due to mixing with additional vector-like quarks, as suggested in ref. [59], thereby increasing the W' branching ratios into multiboson final states. (The decrease in W' cross section is compensated by a larger g_R .) We also note that direct $W' \rightarrow q\bar{q}$ decays, with the two quarks tagged as boson jets, have also been proposed as additional contributions to the ATLAS JJ excess [60]. By considering the efficiency plots in ref. [1] and assuming for simplicity that the tagging variables \sqrt{y} , N_{trk} and m_J are uncorrelated, we estimate that the tagging efficiency for light jets (ϵ_j) is 1/40 of the efficiency for true boson jets (ϵ_V). Therefore, the $W' \rightarrow q\bar{q}$ signal will be suppressed by a factor $(\epsilon_j/\epsilon_V)^2 = 1/1600$ and, likely, contributes negligibly to a possible signal. (The $W' \rightarrow jj$ signal would be comparable to $W' \rightarrow WZ$ if $\epsilon_j = \epsilon_V/5$.) The contribution of $W' \rightarrow t\bar{b}$ with the top and bottom quark jets mistagged as boson jets is expected to be subdominant, because $\sigma(W' \rightarrow t\bar{b}) \leq 40$ fb [42], therefore if we assume a mistagging efficiency $\epsilon_b = \epsilon_V/40$ for b -quark jets the possible contribution is marginal.

The ATLAS diboson excess remains an interesting hint for new physics at the LHC, and for sure new run 2 data will bring light on it, settling the issue of whether this peak, if a real effect, is a diboson resonance or something more complex. For a W' mass of 2 TeV, the cross section at 13 TeV is approximately 7 times higher than at 8 TeV, making up for the smaller luminosity already collected in 2015. The new measurements at 13 TeV [11–15] are yet inconclusive (although they seem to disfavour the possibility of a $R \rightarrow JJ$ resonance), and more data and refined analyses are needed to draw a definite conclusion. Whatever the final outcome of the new measurements is, we have shown in this paper that the scalar sector of models with an extra $SU(2)_R$ provides a rich variety of multiboson signals that are worth exploring in collider experiments.

Acknowledgements

We thank J. Collins, M. Pérez-Victoria and J. Santiago for useful comments. This work has been supported by *Fundação para a Ciência e a Tecnologia* (FCT, Portugal) under the project UID/FIS/00777/2013, by MINECO (Spain) project FPA2013-47836-C3-2-P and by Junta de Andalucía project FQM 101.

References

- [1] G. Aad *et al.* [ATLAS Collaboration], arXiv:1506.00962 [hep-ex].

- [2] V. Khachatryan *et al.* [CMS Collaboration], JHEP **1408** (2014) 173 [arXiv:1405.1994 [hep-ex]].
- [3] V. Khachatryan *et al.* [CMS Collaboration], JHEP **1408** (2014) 174 [arXiv:1405.3447 [hep-ex]].
- [4] G. Aad *et al.* [ATLAS Collaboration], Eur. Phys. J. C **75** (2015) 5, 209 [Erratum Eur. Phys. J. C **75** (2015) 370] [arXiv:1503.04677 [hep-ex]].
- [5] G. Aad *et al.* [ATLAS Collaboration], Eur. Phys. J. C **75** (2015) 69 [arXiv:1409.6190 [hep-ex]].
- [6] V. Khachatryan *et al.* [CMS Collaboration], arXiv:1506.01443 [hep-ex].
- [7] CMS Collaboration, Report CMS-PAS-EXO-14-010.
- [8] J. A. Aguilar-Saavedra, JHEP **1510** (2015) 099 [arXiv:1506.06739 [hep-ph]].
- [9] J. Hisano, N. Nagata and Y. Omura, Phys. Rev. D **92** (2015) 5, 055001 [arXiv:1506.03931 [hep-ph]]; H. S. Fukano, M. Kurachi, S. Matsuzaki, K. Terashi and K. Yamawaki, Phys. Lett. B **750** (2015) 259 [arXiv:1506.03751 [hep-ph]]; D. B. Franzosi, M. T. Frandsen and F. Sannino, arXiv:1506.04392 [hep-ph]; L. Bian, D. Liu and J. Shu, arXiv:1507.06018 [hep-ph]; K. Cheung, W. Y. Keung, P. Y. Tseng and T. C. Yuan, arXiv:1506.06064 [hep-ph]; Y. Gao, T. Ghosh, K. Sinha and J. H. Yu, Phys. Rev. D **92** (2015) 5, 055030 [arXiv:1506.07511 [hep-ph]]; A. Thamm, R. Torre and A. Wulzer, arXiv:1506.08688 [hep-ph]; J. Brehmer, J. Hewett, J. Kopp, T. Rizzo and J. Tattersall, JHEP **1510** (2015) 182 [arXiv:1507.00013 [hep-ph]]; Q. H. Cao, B. Yan and D. M. Zhang, arXiv:1507.00268 [hep-ph]; G. Cacciapaglia and M. T. Frandsen, Phys. Rev. D **92** (2015) 055035 [arXiv:1507.00900 [hep-ph]]; T. Abe, R. Nagai, S. Okawa and M. Tanabashi, Phys. Rev. D **92** (2015) 5, 055016 [arXiv:1507.01185 [hep-ph]]; J. Heeck and S. Patra, Phys. Rev. Lett. **115** (2015) 12, 121804 [arXiv:1507.01584 [hep-ph]]; T. Abe, T. Kitahara and M. M. Nojiri, arXiv:1507.01681 [hep-ph]; A. Carmona, A. Delgado, M. Quirs and J. Santiago, JHEP **1509** (2015) 186 [arXiv:1507.01914 [hep-ph]]; H. S. Fukano, S. Matsuzaki and K. Yamawaki, arXiv:1507.03428 [hep-ph]; L. A. Anchordoqui, I. Antoniadis, H. Goldberg, X. Huang, D. Lust and T. R. Taylor, Phys. Lett. B **749** (2015) 484 [arXiv:1507.05299 [hep-ph]]; K. Lane and L. Prichett, arXiv:1507.07102 [hep-ph]; A. E. Faraggi and M. Guzzi, arXiv:1507.07406 [hep-ph]; M. Low, A. Tesi and L. T. Wang, Phys. Rev. D **92** (2015) 8, 085019 [arXiv:1507.07557 [hep-ph]]; P. Arnan, D. Espriu and F. Mescia, arXiv:1508.00174 [hep-ph]; P. S. Bhupal Dev and R. N. Mohapatra, Phys. Rev. Lett. **115** (2015) 18, 181803 [arXiv:1508.02277 [hep-ph]]; A. Dobado, F. K. Guo

- and F. J. Llanes-Estrada, arXiv:1508.03544 [hep-ph]; F. F. Deppisch, L. Graf, S. Kulkarni, S. Patra, W. Rodejohann, N. Sahu and U. Sarkar, arXiv:1508.05940 [hep-ph]; U. Aydemir, D. Minic, C. Sun and T. Takeuchi, arXiv:1509.01606 [hep-ph]; R. L. Awasthi, P. S. B. Dev and M. Mitra, arXiv:1509.05387 [hep-ph]; T. Li, J. A. Maxin, V. E. Mayes and D. V. Nanopoulos, arXiv:1509.06821 [hep-ph]. P. Ko and T. Nomura, arXiv:1510.07872 [hep-ph].
- [10] G. Aad *et al.* [ATLAS Collaboration], arXiv:1512.05099 [hep-ex].
- [11] ATLAS collaboration, ATLAS-CONF-2015-073.
- [12] ATLAS collaboration, ATLAS-CONF-2015-075.
- [13] ATLAS collaboration, ATLAS-CONF-2015-068.
- [14] ATLAS collaboration, ATLAS-CONF-2015-071.
- [15] CMS Collaboration [CMS Collaboration], CMS-PAS-EXO-15-002.
- [16] C. W. Chiang, H. Fukuda, K. Harigaya, M. Ibe and T. T. Yanagida, JHEP **1511** (2015) 015 [arXiv:1507.02483 [hep-ph]]; G. Cacciapaglia, A. Deandrea and M. Hashimoto, Phys. Rev. Lett. **115** (2015) 17, 171802 [arXiv:1507.03098 [hep-ph]]; V. Sanz, arXiv:1507.03553 [hep-ph]; C. H. Chen and T. Nomura, Phys. Lett. B **749** (2015) 464 [arXiv:1507.04431 [hep-ph]]; Y. Omura, K. Tobe and K. Tsumura, Phys. Rev. D **92** (2015) 5, 055015 [arXiv:1507.05028 [hep-ph]]; W. Chao, arXiv:1507.05310 [hep-ph]; C. Petersson and R. Torre, arXiv:1508.05632 [hep-ph]; C. H. Chen and T. Nomura, arXiv:1509.02039 [hep-ph]; D. Aristizabal Sierra, J. Herrero-Garcia, D. Restrepo and A. Vicente, arXiv:1510.03437 [hep-ph].
- [17] B. C. Allanach, B. Gripaios and D. Sutherland, Phys. Rev. D **92** (2015) 5, 055003 [arXiv:1507.01638 [hep-ph]]; D. Kim, K. Kong, H. M. Lee and S. C. Park, arXiv:1507.06312 [hep-ph]; S. P. Liew and S. Shirai, arXiv:1507.08273 [hep-ph]; H. Terazawa and M. Yasue, arXiv:1508.00172 [hep-ph]; D. Gonalves, F. Krauss and M. Spannowsky, Phys. Rev. D **92** (2015) 5, 053010 [arXiv:1508.04162 [hep-ph]]; S. Fichet and G. von Gersdorff, arXiv:1508.04814 [hep-ph]; L. Bian, D. Liu, J. Shu and Y. Zhang, arXiv:1509.02787 [hep-ph]; A. Sajjad, arXiv:1511.02244 [hep-ph]; B. Bhattacharjee, P. Byakti, C. K. Khosa, J. Lahiri and G. Mendiratta, arXiv:1511.02797 [hep-ph].
- [18] B. C. Allanach, P. S. B. Dev and K. Sakurai, arXiv:1511.01483 [hep-ph].

- [19] G. Aad *et al.* [ATLAS Collaboration], Eur. Phys. J. C **73** (2013) 1, 2263 [arXiv:1210.4826 [hep-ex]].
- [20] S. Chatrchyan *et al.* [CMS Collaboration], Phys. Rev. Lett. **110** (2013) 14, 141802 [arXiv:1302.0531 [hep-ex]].
- [21] T. Aaltonen *et al.* [CDF Collaboration], Phys. Rev. Lett. **111** (2013) 3, 031802 [arXiv:1303.2699 [hep-ex]].
- [22] V. Khachatryan *et al.* [CMS Collaboration], Phys. Lett. B **747** (2015) 98 [arXiv:1412.7706 [hep-ex]].
- [23] F. F. Deppisch, T. E. Gonzalo, S. Patra, N. Sahu and U. Sarkar, Phys. Rev. D **90** (2014) 5, 053014 [arXiv:1407.5384 [hep-ph]].
- [24] M. Heikinheimo, M. Raidal and C. Spethmann, Eur. Phys. J. C **74** (2014) 10, 3107 [arXiv:1407.6908 [hep-ph]].
- [25] J. A. Aguilar-Saavedra and F. R. Joaquim, Phys. Rev. D **90** (2014) 11, 115010 [arXiv:1408.2456 [hep-ph]].
- [26] V. Khachatryan *et al.* [CMS Collaboration], Eur. Phys. J. C **74** (2014) 11, 3149 [arXiv:1407.3683 [hep-ex]].
- [27] C. H. Chen and T. Nomura in ref. [16]
- [28] G. Aad *et al.* [ATLAS Collaboration], arXiv:1509.00672 [hep-ex].
- [29] J. de Blas, M. Chala, M. Perez-Victoria and J. Santiago, JHEP **1504** (2015) 078 [arXiv:1412.8480 [hep-ph]].
- [30] J. C. Pati and A. Salam, Phys. Rev. D **10**, 275 (1974) [Erratum-ibid. D **11**, 703 (1975)]; R. N. Mohapatra and J. C. Pati, Phys. Rev. D **11**, 2558 (1975); G. Senjanovic and R. N. Mohapatra, Phys. Rev. D **12**, 1502 (1975).
- [31] G. Senjanovic, Nucl. Phys. B **153** (1979) 334.
- [32] G. Ecker, W. Grimus and H. Neufeld, Nucl. Phys. B **247** (1984) 70.
- [33] G. C. Branco, P. M. Ferreira, L. Lavoura, M. N. Rebelo, M. Sher and J. P. Silva, Phys. Rept. **516** (2012) 1 [arXiv:1106.0034 [hep-ph]].
- [34] R. N. Mohapatra, G. Senjanovic and M. D. Tran, Phys. Rev. D **28** (1983) 546; F. J. Gilman and M. H. Reno, Phys. Lett. B **127** (1983) 426; Phys. Rev. D **29** (1984) 937; G. Ecker and W. Grimus, Nucl. Phys. B **258** (1985) 328.

- [35] M. E. Pospelov, Phys. Rev. D **56** (1997) 259.
- [36] B. A. Dobrescu and Z. Liu, JHEP **1510** (2015) 118.
- [37] S. Chatrchyan *et al.* [CMS Collaboration], Phys. Lett. B **722** (2013) 207 [arXiv:1302.2892 [hep-ex]].
- [38] V. Khachatryan *et al.* [CMS Collaboration], arXiv:1510.01181 [hep-ex].
- [39] V. Khachatryan *et al.* [CMS Collaboration], arXiv:1511.03610 [hep-ex].
- [40] K. A. Olive *et al.* [Particle Data Group Collaboration], Chin. Phys. C **38** (2014) 090001.
- [41] D. Duffy and Z. Sullivan, Phys. Rev. D **86** (2012) 075018 [arXiv:1208.4858 [hep-ph]].
- [42] V. Khachatryan *et al.* [CMS Collaboration], arXiv:1509.06051 [hep-ex].
- [43] G. Aad *et al.* [ATLAS Collaboration], Eur. Phys. J. C **75** (2015) 4, 165 [arXiv:1408.0886 [hep-ex]].
- [44] G. Aad *et al.* [ATLAS Collaboration], Phys. Lett. B **743** (2015) 235 [arXiv:1410.4103 [hep-ex]].
- [45] G. Aad *et al.* [ATLAS Collaboration], Phys. Rev. D **91** (2015) 5, 052007 [arXiv:1407.1376 [hep-ex]].
- [46] V. Khachatryan *et al.* [CMS Collaboration], Phys. Rev. D **91** (2015) 5, 052009 [arXiv:1501.04198 [hep-ex]].
- [47] G. Aad *et al.* [ATLAS Collaboration], Phys. Rev. D **90** (2014) 5, 052005 [arXiv:1405.4123 [hep-ex]].
- [48] K. Melnikov and F. Petriello, Phys. Rev. D **74** (2006) 114017 [hep-ph/0609070].
- [49] P. Langacker, M. x. Luo and A. K. Mann, Rev. Mod. Phys. **64** (1992) 87.
- [50] P. Langacker, Rev. Mod. Phys. **81** (2009) 1199 [arXiv:0801.1345 [hep-ph]].
- [51] T. G. Rizzo, hep-ph/0610104.
- [52] P. Langacker and S. U. Sankar, Phys. Rev. D **40** (1989) 1569.
- [53] J. Polak and M. Zralek, Nucl. Phys. B **363** (1991) 385.
- [54] J. Chay, K. Y. Lee and S. h. Nam, Phys. Rev. D **61** (2000) 035002 [hep-ph/9809298].

- [55] K. Hsieh, K. Schmitz, J. H. Yu and C.-P. Yuan, Phys. Rev. D **82** (2010) 035011 [arXiv:1003.3482 [hep-ph]].
- [56] J. A. Aguilar-Saavedra, R. Benbrik, S. Heinemeyer and M. Pérez-Victoria, Phys. Rev. D **88** (2013) 9, 094010 [arXiv:1306.0572 [hep-ph]].
- [57] N. G. Deshpande, J. F. Gunion, B. Kayser and F. I. Olness, Phys. Rev. D **44** (1991) 837.
- [58] J. F. Gunion, J. Grifols, A. Mendez, B. Kayser and F. I. Olness, Phys. Rev. D **40** (1989) 1546.
- [59] J. H. Collins and W. H. Ng, arXiv:1510.08083 [hep-ph].
- [60] B. A. Dobrescu and P. J. Fox, arXiv:1511.02148 [hep-ph].